Sensors and Materials, Vol. 23, No. 7 (2011) 397–417
MYU Tokyo

S & M 0855

Design, Fabrication, and Evaluation of Highly Sensitive Compact Chemical Sensor System Employing a Microcantilever Array and a Preconcentrator

Takashi Mihara*, Tsuyoshi Ikehara[1], Mitsuo Konno[1], Sunao Murakami[1], Ryutaro Maeda[1], Tadashi Fukawa[2] and Mutsumi Kimura[2]

Future Creation Laboratory, Olympus Corporation,
2-3 Kuboyama-cho, Hachiouji, Tokyo 192-8512, Japan
[1]National Institute of Advanced Industrial Science and Technology,
1-2 Namiki, Tsukuba, Ibaraki 305-8564, Japan
[2]Faculty of Textile Science & Technology, Shinshu University,
Tokida 3-15-1, Ueda, Nagano 386-8567, Japan

(Received January 17, 2011; accepted April 12, 2011)

Key words: chemical sensor, microcantilever, cantilever array, preconcentrator, poly-butadiene, acrylonitrile-co-butadiene, acetone, toluene, xylene

We developed a highly sensitive compact chemical sensor system employing a polymer-coated microcantilever sensor array and a thermal preconcentrator. The design, structure, fabrication, and experiment results are reported here. This sensor system had 1) a sub-ppb detection limit concentrated by a preconcentrator and 2) analytical function by thermal desorption of the preconcentrator and multiple cantilevers (acting as the mass sensor) with different polymers. The preconcentrator contained 0.03 g of carbon fiber, and absorption/desorption were controlled by the temperature from room temperature to 520°C. The sample gas was introduced into the preconcentrator using a miniature air pump at a flow rate of 2.0 L/min. Four silicon microcantilevers in one silicon chip fabricated by micro-electromechanical systems (MEMS) technology were packaged in a ceramic flat package and driven by a PZT actuator plate mounted in the package. Using the 4th vibration mode (resonant frequency: 764 kHz) of a polybutadiene (2.52 μm thick)-coated cantilever, the sensitivity was 514 Hz/ppm for toluene and 850 Hz/ppm for p-xylene with a 5 min preconcentration time. The preconcentration factor and system efficiency of sensing were estimated to be 830 and 0.78, respectively, for toluene. The estimated detection limit of the sensor system was less than 1 ppb for toluene

*Corresponding author: e-mail: t_mihara@mmc.or.jp

and p-xylene with a 10 L sample volume, which was good enough for application to environmental monitoring. Separate detection of the mixed toluene and p-xylene was also achieved in the form of different time peaks during the heating preconcentrator operation.

1. Introduction

The development of a chemical sensor system to detect volatile organic compound (VOC) species has been receiving much attention for environmental monitoring and ultrafast medical diagnostics. To date, the widely used sensor to detect VOCs has been the metal oxide semiconductor (MOS) sensor; however, it is difficult to analyze the VOC elements owing to the relatively poor selectivity of compounds. Quartz crystal microbalance (QCM) and surface acoustic wave (SAW) devices with sensing films have also been widely investigated; however, they are also difficult to integrate with electronic devices into a smart sensor. New highly sensitive micromass sensors including a microcantilever have recently been developed.[1–4] However, previous investigations show a somewhat low sensitivity, such as 0.01 Hz/ppm for ethanol and 0.1 Hz/ppm for toluene.

We have been developing an integrated chemical analysis system with focus on the resonant micromass sensor for this purpose. We have reported studies on the mass sensitivity of the silicon microcantilever with high resonant modes,[5,6] sensing films using copolymer-based elastic polymers,[7] and the first prototype sensor system.[8] We consider that silicon micromass sensors with cantilevers are potential smart sensors because they can be easily integrated with electronic devices to provide intelligent functions in a chemical sensor system. To increase the sensitivity, we used a preconcentrator. To obtain the analytical function, we utilized the desorption characteristics of a heating preconcentrator and cantilever arrays.[9,10] We also reported the estimation of concentration factors and system efficiencies using basic formulas for the cantilever-type chemical sensor system.[11] Several previous investigations to combine a preconcentrator with SAW devices and QCM-type sensors have been reported to date. With the use of the TENAX-TA (polymer beads based on 2,6-diphenyl-p-phenylene oxide by Teijin)-filled preconcentrator and 433 MHz SAW sensor, the detection limit for toluene was reported to be 0.08 ppm and that for ethanol was 33 ppm after 3 min of concentration.[12,13] Another report showed the separation of the components with the thermal preconcentrator combined with QCM devices.[14]

In this study, we report the design, fabrication and evaluation results of a newly developed sub-ppb-detectable sensor system possessing both preconcentration and analytical functions. This report contains the detailed design method, system setup, and experimental results for the compact sensor system, as an extension of the previous report.[11] A part of § 2 (including Figs. 1, 3, and 6) was reconstructed from Figs. 1–3 in ref. 11 to maintain the consistency of mathematical notations and to demonstrate the system improvement.

2. Design, Materials, and Methods

2.1 *Design of sensor system*

The potential applications of our chemical sensor system are in environmental monitoring and medicine. The environmental monitoring requires toxic VOC (including toluene and xylene) sensing at extremely low concentration of sub-ppb order for a relatively large air volume (more than 10 L). Medical application requires the detection of specific gases, for example, acetone in a few liters of sample to diagnose diabetes.[15] We also require compact size and low-cost operation in addition to on-site measurement in the sensing field. These requirements allow the sensor system to be equipped with an analytical function and a preconcentrator. Thus, our sensor system comprised an air pump, a preconcentrator, and a cantilever array as a sensing device, as shown in Fig. 1. The sample gas was introduced into the preconcentrator by pumping at room temperature. Then, the temperature of the preconcentrator was gradually increased by the heater, and the desorbed gases at a specific temperature were delivered into a sensor chamber with pure nitrogen carrier gas. This desorbed gas was detected by a cantilever array coated with different polymers under controlled temperature. The shifts of frequency appeared at different times, as shown in Fig. 1.

We introduced detailed descriptions of important formulas, including those for the frequency shift of the cantilever sensor, the condition of oscillation for multiple cantilevers, preconcentration and analysis of VOC, the definition of sensitivity, efficiencies and concentration factor of our system, and the detection limit, in addition to those in the previous report.[11] On the basis of these formulas, the sensor system was designed and its performance was evaluated.

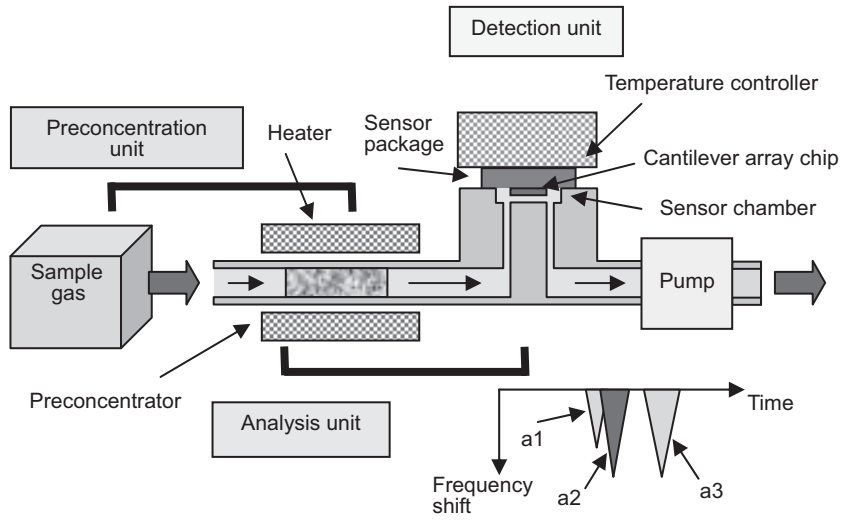

Fig. 1. Sensing concept of our sensor system.

2.1.1 *Sensitivity of cantilever mass sensor*

We chose a microcantilever as a mass-sensing resonator because its characteristics are well known, its fabrication is well established, and its combination with electronic devices is easy. The resonant frequency of the nth flexural mode of resonant frequency f_0 of a cantilever with length L_{Si} and thickness t_{Si} is shown as

$$f_0 = k_n \frac{t_{Si}}{L_{Si}^2} \sqrt{\frac{E_{Si}}{\rho_{Si}}}, \tag{1}$$

where E_{Si}, ρ_{Si}, and k_n are Young's modulus, the density of silicon, and the coefficient dependent on mode n, respectively.[16] After the deposition of polymers that act as VOC sensing materials, the resonant frequency f_P of the nth mode vibration is reduced by the change in the cantilever's mass as

$$f_P = f_0 - \frac{1}{2} f_0 \frac{\sigma_{Poly}}{\sigma_{Si} + \sigma_{Pad}}, \tag{2}$$

where σ_{Poly}, σ_{Si}, and σ_{Pad} (kg/m^2) are the surface densities of the polymer, silicon, and adhesive layer between them, respectively.

The frequency shift Δf_a of the polymer-coated cantilever after exposure to the diluted VOC "a" is described as

$$\Delta f_a = -\frac{1}{2} f_P \frac{\Delta m_c}{m_c}, \tag{3}$$

where m_c is the mass of the cantilever and Δm_c is the change in m_c upon VOC exposure. Equations (2) and (3) are derived from the differential of eq. (1). The Δm_c is estimated using a product of K_a, the concentration of the gas phase, and the volume of polymer as

$$\Delta m_c = \frac{K_a C_a M_a A_c t_{Poly}}{0.0224}, \tag{4}$$

where K_a is the distribution factor (or K-factor) of VOC for the related polymer, which is defined as the ratio of the volume concentrations of VOC in the polymer to that in the surrounding gas in the equilibrium state. C_a and M_a are the concentration of VOC in mole ratio and the mole weight of diluted VOC, respectively. A_c and t_{Poly} are the area of the cantilever and the polymer thickness, respectively. The mole volume in the ideal gas state is 0.0224 m^3, which was used to transform the mole ratio to the volume ratio. Then Δf_a is expressed, using the surface densities of the cantilever, as

$$\Delta f_a = -\frac{1}{2} f_P \frac{K_a C_a M_a t_{Poly}}{0.0224 \cdot 10^6 (\sigma_{Si} + \sigma_{Pad} + \sigma_{Poly})}. \tag{5}$$

Hence the sensitivity of the cantilever sensor s_a (Hz/ppm), defined as the ratio of the change in frequency to the concentration in ppm, is shown as

$$s_a = -\frac{1}{2} f_{\mathrm{P}} \frac{K_a M_a t_{\mathrm{Poly}}}{0.0224 \cdot 10^6 \left(\sigma_{\mathrm{Si}} + \sigma_{\mathrm{Pad}} + \sigma_{\mathrm{Poly}}\right)}. \tag{6}$$

The sensitivity is proportional to the resonant frequency, K_a, t_{Poly}, and the inverse of the surface density of the cantilever.

2.1.2 *Design of oscillation circuit of cantilever array*

The design of an oscillation circuit of cantilever sensors is described. Figure 2 shows the schematic of the two-cantilever oscillation system. This circuit contains two cantilevers with stress gauges, two front-end amplifiers with gain g_i (i = 1, 2), a multiplexer (MPX), a phase shifter (PS), a bandpass filter (BPF), and a PZT plate as an actuator. First, we explain the design for one cantilever sensor. The driving signal $p_i(t)$ fed to the PZT actuation plate is expressed using the amplitude P_{0i}, the driving frequency f_{PZT}, and the phase χ_i of driving signal as

$$p_i(t) = P_{0i} \sin\left(2\pi f_{\mathrm{PZT}} t + \chi_i\right). \tag{7}$$

When MPX selects the ith cantilever, the signal $u_i(t)$ of the piezoresistive gauge with the specific vibration mode of the ith cantilever is expressed with the amplitude U_{0i}, the resonant frequency f_i, and the phase shift φ_i as

$$u_i(t) = U_{0i} \sin\{2\pi \left[f_i(1 + \beta_i \Delta T_{\mathrm{c}})\right]t + \varphi_i + \delta\varphi_i\}. \tag{8}$$

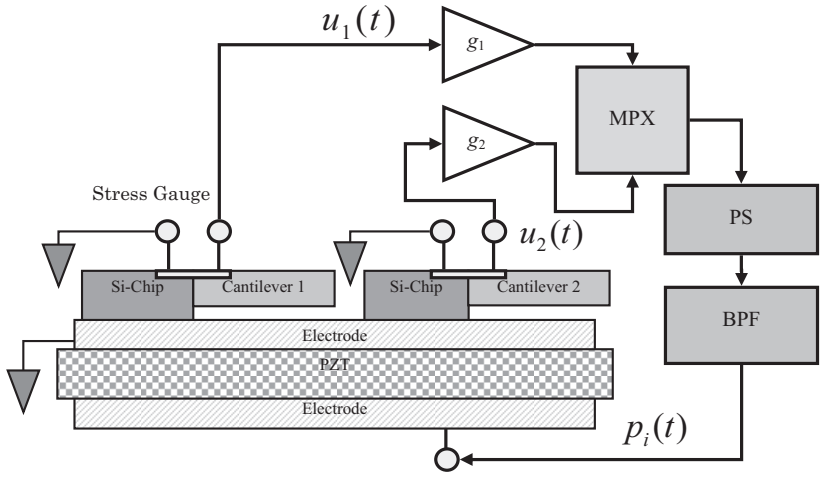

Fig. 2. Schematic of two-cantilever oscillation system.

Equation (8) also includes the temperature coefficient β_i, the change in cantilever temperature ΔT_c, and the phase variation $\delta\varphi_i$. The temperature dependence of frequency produced by β_i is a major cause of the frequency drift and should be compensated by the measurement of chip temperature.[17] The $\delta\varphi_i$ produces the short-range variation of frequency that determines the detection limit of chemical sensors.

We designed the oscillation circuit of the cantilever subject to the following three items.

(1) The f_{PZT} is adjusted by the central frequency of BPF to match the resonant frequency of the cantilever as

$$f_{PZT} = f_i\,(1 + \beta_i \Delta T_c). \tag{9}$$

(2) The total gain G_i of the circuit, including g_i of the front-end amplifier, is set to be larger than the ratio of P_{0i} to U_{0i}:

$$\frac{P_{0i}}{U_{0i}} \leq G_i\,. \tag{10}$$

The g_i is adjusted to the specific value for the ith cantilever and G_i is automatically adjusted by AGC to an adequate value of $G_i = P_{0i}/U_{0i}$ when stable oscillation occurs.

(3) The phase π_i of PS is adjusted such that the sum of phases φ_i, χ_i, π_i, and a phase θ_i of other circuits including the amplifier, BPF, and MPX is a multiple of 2π as

$$\varphi_i + \chi_i + \pi_i + \theta_i = 2\pi I, \tag{11}$$

where I is an integer. In actual experiment, the central frequency of BPF is adjusted to obtain the maximum values of P_{0i}. After that, π_i of PS is adjusted to obtain the maximum values of U_{0i}. Then the stable resonant vibration of the cantilever occurs. Note that the G_i varies with many mechanical parameters including the efficiency/coupling factors of PZT, the piezoresistive gauge, and the adhesive glue.

We now explain the case of the cantilever array. We applied electrical multiplexing to drive multiple cantilevers, because the oscillation circuit became complicated, making it difficult to obtain stable oscillation. After the switching of the sensor signal from i to i+1 using MPX, $u_i(t)$ is altered to $u_{i+1}(t)$ by the specific U_{0i+1}, f_{i+1}, and φ_{i+1} for each cantilever, as shown in eq. (8) . The design and oscillation conditions should also be satisfied on the (i+1)th cantilever, as shown in eqs. (9) to (11). We found that U_{0i}, f_i, and φ_i for each cantilever with polymer are not the same, and these values should be adjusted after multiplexing. Then, we utilized a presetting circuit with memory, as described in § 2.2.3.

2.1.3 *Preconcentration*

We applied a preconcentrator to improve the detection limit of the system at the ppb level. Figure 3 shows the schematic diagram of the flow of the gas sample from the sample bag to the sensor. The VOC gas with component "a" and mass m_a (kg) in the gas

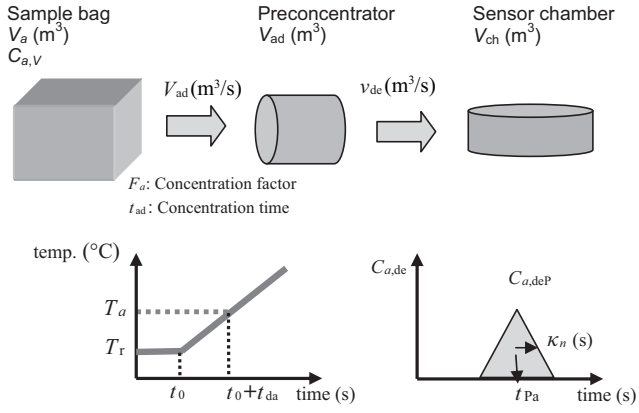

Fig. 3. Block diagram of gas flow from sample bag to sensor.

state is diluted in volume V_a (m^3) with concentration $C_{a,V}$, as shown in Fig. 3. When the gas of V_a is introduced to the preconcentrator of V_{ad} (m^3) with flow of a volume velocity of v_{ad} (m^3/s), component "*a*" will be adsorbed in the adsorption material. The mass of component "*a*" in the preconcentrator $m_{a,ad}$ (kg) is reduced by the preconcentrator efficiency η_a as

$$m_{a,\mathrm{ad}} = \eta_a m_a = \eta_a \frac{M_a V_a C_{a,V}}{0.0224}. \tag{12}$$

Then, $(1-\eta_a)$ represents for the part that escapes from the preconcentrator when sample gas is adsorbed.

2.1.4 *Sensing response of VOC by sensor system with preconcentrator*

The adsorbed VOC in the preconcentrator is desorbed by heating and streamed to the sensor chamber by high-purity nitrogen carrier gas with a volume velocity of v_{de} (m^3/s), as shown in Fig. 3. The peak time t_{Pa} (*s*) of component "*a*" measured with the sensor is presented as

$$t_{\mathrm{Pa}} = t_0 + \frac{T_a - T_{\mathrm{r}}}{r_{\mathrm{t}}} + \frac{S_{\mathrm{t}} L_{\mathrm{t}}}{v_{\mathrm{de}}} + \frac{V_{\mathrm{ch}}}{v_{\mathrm{de}}}, \tag{13}$$

where $t_0(s)$ is the start time of heating, as shown in Fig. 3. The second term stands for the time taken to reach desorption t_{da} (*s*), in which T_r, T_a (°C), and r_t (°C/s) are room temperature, the desorption temperature of VOC "*a*," and the heating rate of the preconcentrator, respectively, as shown in Fig. 3. The third term is the delivery time from the preconcentrator to the sensor chamber by the carrier gas, in which S_t (m^2) is

the cross-sectional area of the gas tube, L_t (m) the length of the tube, and v_{de} (m^3/s) the volume velocity of the carrier gas. The fourth term is the filling time of VOC in the sensor chamber with volume V_{ch} (m^3). If the sample gas is a mixture of several VOCs, multiple peaks are observed because of the difference in T_a among VOCs. The T_a is determined as the extrapolation value at y-axis of $1/v_{de}$ dependence of t_{Pa}.

The desorption response of absorbed gas is explained on the basis of the theory of temperature-programmed desorption (TPD).[18] The time t dependence of desorption molecules $N_d(t)$ (molecules/s) is expressed with the absorbed surface amount Ω_z (molecules/cm^2), the reaction order of desorption z, the absorption rate γ_z (molecules/s), the desorption energy E_a (eV), and the Boltzmann constant k_B as

$$N_d(t) = -\frac{d\Omega_z}{dt} = \gamma_z \Omega_z^z \exp\left[\frac{E_a}{k_B (T_a + 273.15)}\right]. \quad (14)$$

However, Ω_z in eq. (14) is solved by the numerical integration with adsorption temperature, and $N_d(t)$ is solved by the numerical differential, which is too complicated to fit an actual sensing response curve to analyze the multiple components. Therefore, we use the linear combination of several Gaussian functions as

$$\Delta f_{mix}(t) = \Delta f_{0mix} + \sum_{j=1}^{N} \Delta f_{Pa,j} \exp\left[-\frac{(t - t_{Pa,j})^2}{\kappa_{a,j}^{\ 2}}\right], \quad (15)$$

to explain the actual sensor response. Hence, $\Delta f_{mix}(t)$, Δf_{0mix}, $\Delta f_{Pa,j}$, $t_{Pa,j}$, and $\kappa_{a,j}$ are the response of frequency shift by mixed VOCs, the baseline of $\Delta f_{mix}(t)$, the peak value of frequency shift for the jth component, the peak time for the jth (or "a") component, and the standard deviation for the jth (or "a") component, respectively. Note that t_{Pa} in eq. (13) is equal to $t_{Pa,j}$ when $j = 1$.

The final sensing mass $m_{a,de}$ (kg) of component "a" detected by the sensor is calculated with the desorption response as

$$m_{a,de} = \frac{M_a}{0.0224} v_{de} \sum_{\Delta t_{de}} \Delta t_{de} C_{a,de}(t) = \frac{M_a}{0.0224} v_{de} \sum_{\Delta t_{de}} \Delta t_{de} s_a \Delta f_a(t), \quad (16)$$

where $\Delta t_{de}(s)$ is time interval of sensing, and $C_{a,de}(t)$ is the observed concentration of VOC by the cantilever sensor at time t. This $m_{a,de}$ is a part of the mass $m_{a,ad}$ of absorbed VOC in the preconcentrator; then, $m_{a,de}$ is presented by another efficiency ξ_a as

$$m_{a,ad} = \xi_a m_{a,ad} = \xi_a \eta_a m_a. \quad (17)$$

We can evaluate the total efficiency $\xi_a \eta_a$ of the system by taking the ratio of $m_{a,de}$ to m_a. The concentration factor $F_{a,V}$ of a sensor system is defined using the ratio of $C_{a,deP}$ (peak value of $C_{a,de}(t)$ in Fig. 3) to $C_{a,V}$ as

$$F_{a,V} = \frac{C_{a,\mathrm{deP}}}{C_{a,V}}\ , \tag{18}$$

which is proportional to V_a. In practical use, the sample volume is determined from the volume of the sample bag or the time of aspiration t_{ad} (s) into the preconcentrator by an air pump. Then, we defined the system sensitivity $S_{a,10\mathrm{L}}$ (Hz/ppm when V_a = 10 L) as

$$S_{a,10\mathrm{L}} = \frac{\Delta f_{a,10\mathrm{L}}}{C_{a,10\mathrm{L}}} = F_{a,10\mathrm{L}} s_a, \tag{19}$$

where $\Delta f_{a,10\mathrm{L}}$ and $C_{a,10\mathrm{L}}$ are the measured frequency shift and the concentration when V_a = 10 L, and $F_{a,10\mathrm{L}}$ is the measured concentration factor when V_a = 10 L.

Finally, the detection limit $DL_{a,10\mathrm{L}}$ (ppb when V_a = 10 L) is derived from the standard variation λ of Δf_a in a short time and $S_{a,10\mathrm{L}}$ as

$$DL_{a,10\mathrm{L}} = \frac{3\lambda}{10^{-3} S_{a,10\mathrm{L}}} = \frac{3\lambda}{10^{-3} F_{a,10\mathrm{L}} s_a}\ , \tag{20}$$

where 10^{-3} is used to transform ppm to ppb. To obtain a low detection limit, efforts to reduce λ, including the high quality factor of the resonator, and to reduce electric noise are essential, in addition to the high sensitivity.

We expressed the important formulas of our sensor system described above for the purpose of designing the sensor system. We used eqs. (1) to (6) to analyze and design a cantilever sensor, eqs. (7) to (11) to design oscillation circuits and temperature compensation, and eqs. (12) to (20) to design the operation parameters and analyze the performance.

2.2 *System components*

2.2.1 *Cantilever sensors and packaging*

Silicon cantilevers were fabricated by microfabrication techniques from an SOI wafer.[5] The length, width, and thickness of the cantilever were 500, 100, and 5 μm, respectively. A set of bridged piezoresistive stress gauges was formed at the root of the cantilever from the p-type layer in the n-type active layer employing boron implantation and thermal diffusion. The substrate under the cantilever was removed by deep RIE from the backside to eliminate the squeezed air damping effect. A gold pattern was formed on the upper surface of the cantilever to obtain an adequate adhesion characteristic with polymers. Eight cantilevers in one silicon chip were packaged in a ceramic flat package and driven by a PZT actuator plate mounted in the package. The silicon chip was adhered to the PZT plate with epoxy, and the PZT plate was mounted on the flat package with epoxy at the four corners and Ag paste at the center, as shown in Fig. 4(a). Four of the eight cantilevers were wire bonded and used as sensors. Figure 4(a) also shows the temperature controller attached to the package.

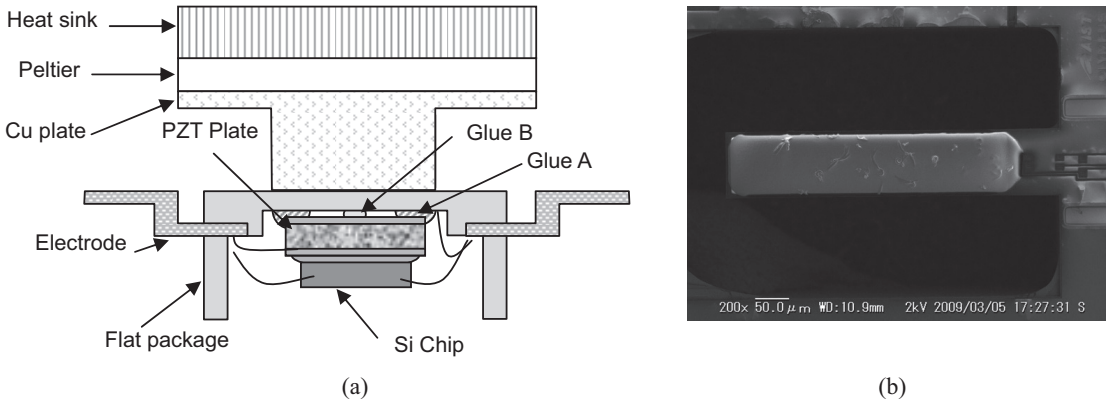

Fig. 4. (a) Flat package of cantilever chip with PZT plate and a temperature controller, (b) SEM image of PBD-coated cantilever.

2.2.2 *Polymer (sensing material)*

Two types of polymer among the elastomer-type materials were used as VOC sensing films in this study. One was poly-butadiene (PBD), which is sensitive to aromatic VOC gases including toluene and xylene. The other was poly(acrylonitrile-co-butadiene) (PAB), which is sensitive to alcohol and acetone. We found that the PBD and PAB films showed fast response to adsorption and desorption while these films were exposed to various VOCs.[7,19] These thin films were deposited on the cantilever by the microdispensing technique. The thicknesses of the PBD and PAB films were controlled from 300 to 2,500 nm by varying the duration of dispensing. A SEM image of the PBD-coated cantilever demonstrates that flat and smooth surfaces were obtained, as shown in Fig. 4(b).

2.2.3 *Oscillation circuit*

The signal from the bridged piezoresistive stress gauge on each cantilever was amplified by a front-end differential amplifier (A), then selected by an electrically programmed MPX and oscillated using a feedback circuit, as shown in Fig. 5. The oscillation circuit consisted of an automatic gain controller (AGC), a PS and a second-order BPF. The f_i, amplitude U_{0i}, and phase φ_i, as presented in eq. (8) for each cantilever (i = 1 to 4), were greatly varied among cantilevers owing to the difference in mechanical characteristics depending on the coated materials, the site of the cantilever in a chip, and the method of PZT mounting, as shown in Fig. 4(a). Therefore, two parameters, namely, 1) the amount of feedback phase shift π_i in eq. (11) and 2) f_i for the i-th cantilever, were stored in the memory on the oscillation circuit board and used when multiplexing to achieve oscillation under the best conditions. Hence, the amplitude U_{0i} was automatically adjusted with AGC. Figure 5 shows the additional AD and DA converters and random access memories (RAMs) in conjunction with PS and BPF to preset and store the feedback phase and the resonance frequency. Thanks to these preset circuits, we could oscillate cantilevers of various sizes, modes and polymer materials.

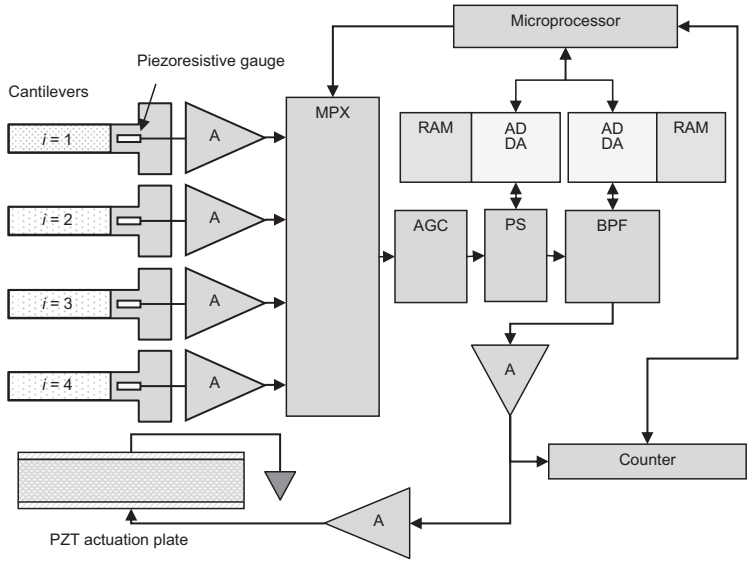

Fig. 5. Block diagram of oscillation circuit with phase and resonant frequency preset at MPX switching.

2.2.4 *Preconcentrator*

A preconcentrator was made of a 6.35-mm-diameter stainless-steel tube, in which 0.03 g of carbon fiber (Kuraray Chemical: maximum surface area of about 2,500 m^2/g) was filled, as shown in Fig. 6. A 1-mm-diameter sheathed heater was wound on the tube with thermal insulation material. This preconcentrator, which is capable of being heated up to 600°C, was installed at the inlet of the sensor chamber to concentrate a sample gas in the sample bag or environmental air directly. To separate the mixed VOCs, the temperature of the preconcentrator was gradually increased at r_t = 1.0 to 1.3°C/s using the programmed DC power supply.

2.2.5 *Total sensor system structure*

Figure 7(a) shows the sensor system including an air pump, a preconcentrator, and a sensor chamber. A Peltier device with an electric fan was installed in the sensor chamber to keep the temperature of the cantilever sensor constant. The temperature of the cantilever sensor was measured using a p-n junction diode fabricated in the same chip.[17] The size of the total system was 280 × 200 × 80 mm^3. Figure 7(b) also shows an electronics case including three electrical circuit boards for oscillation, control, and power units. These circuits included two R8c microcomputers (Renesas Electronics Corporation), and all control commands and measured data were shared with a personal computer (PC) via a universal serial bus (USB) interface. Measurement and analysis

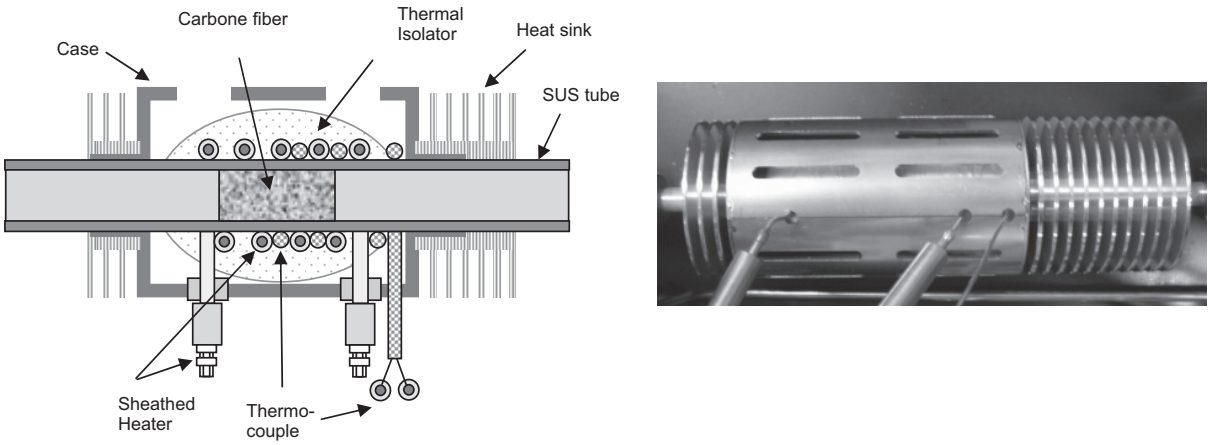

Fig. 6. Preconcentrator: (a) cross-sectional schematic and (b) photograph of covered preconcentrator.

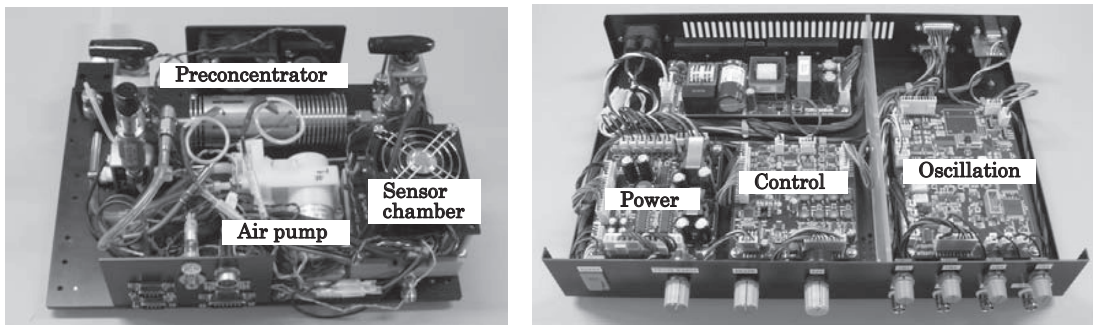

Fig. 7. Photographs of our sensor system: (a) sensor system including air pump, preconcentrator, and sensor chamber; (b) electrical units with three circuit boards.

software was programmed with Visual Basic, in which several design formulas in this paper were implemented to evaluate system parameters. Figure 8(a) shows the airflow diagram of our sensor system shown in Fig. 7(a), in which three-port manual valves (V), a mass flow meter (MFM) and a needle valve are shown. Figure 8(b) shows two measurement steps of an actual application: (1) in preconcentration, a pump pulls the sample gas though a preconcentrator at room temperature, and (2) in detection and analysis, pure nitrogen carrier gas pushes the desorbed VOCs from the heating preconcentrator into the sensor chamber, where a needle valve maintains volume velocity v_{de} of the carrier gas constant with MFM monitoring.

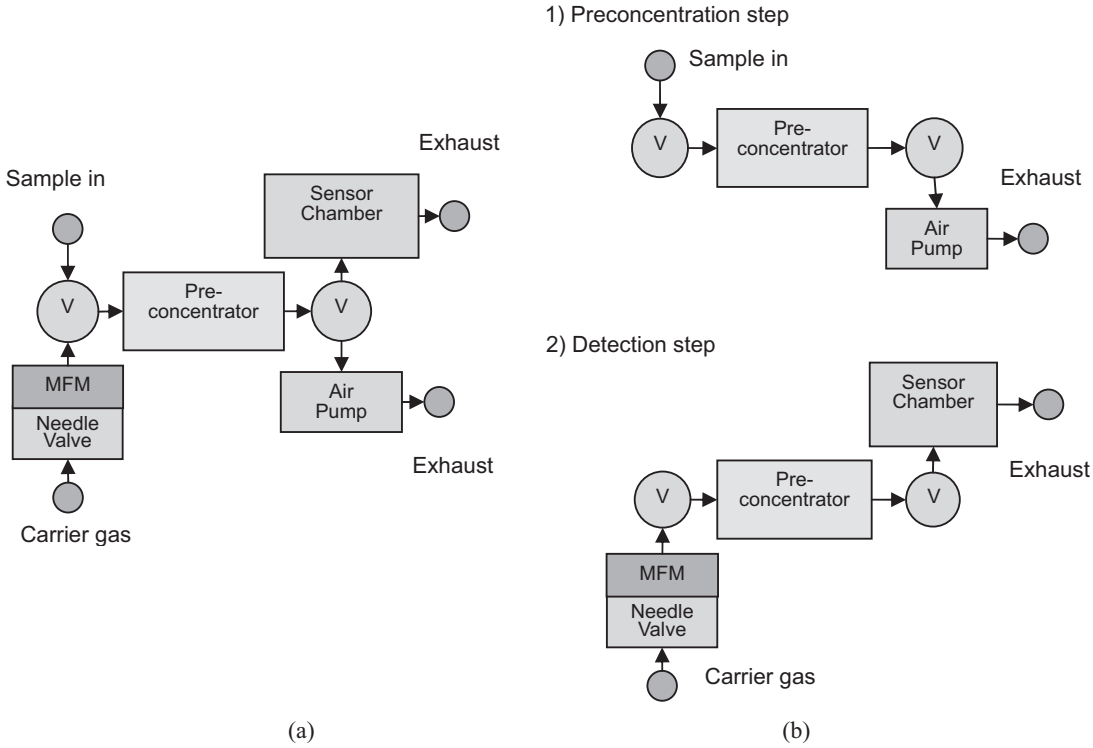

Fig. 8. (a) Configuration of our sensor system. (b) VOC flow in actual operation: 1) preconcentration of sample gas, and 2) analysis and detection.

3. Results

3.1 *Performance of polymer-coated cantilever without preconcentrator*

3.1.1 *Estimations of thickness of polymers*

First, we estimated the thicknesses of polymers as the sensing material. The prepared samples have been described in § 2.2.1 and § 2.2.2, and the polymers were PAB and PBD. We evaluated the 4th mode of resonant frequency f_0 (before coating) and f_P (after coating) to determine the thickness using eqs. (1) to (2). The thickness t_{Si} was determined using f_0 in eq. (1), and t_{Poly} was calculated using eq. (2) from the difference between f_P and f_0 shown in Table 1. Thus, the thicknesses of PBD and PAB were evaluated to be 2,520 and 640 nm, respectively.

3.1.2 *Estimations of sensitivity and K-factor*

Then, we evaluated the C_a dependence of Δf_a for several VOCs to determine the K_a. Figure 9 shows Δf_a for four VOCs without a preconcentrator: (a) 640-nm-thick PAB thin film and (b) 2,520-nm-thick PBD thin film. The drift componet of Δf_a was compensated

Table 1
Sensitivities and K-factors for VOCs for PAB- and PBD-coated cantilevers.

Polymer	f_0 (kHz)	f_{poly} (kHz)	t_{Si} (μm)	t_{Poly} (nm)	Acetone		1-Propanol		Toluene		p-Xylene	
					s_{ace}	K_{ace}	s_{pnl}	K_{pnl}	s_{tol}	K_{tol}	s_{pxy}	K_{pxy}
PAB	911.4	885.2	4.87	640	0.036	605	0.15	2,380	0.25	2,650	0.63	5,800
PBD	862.5	764.3	4.69	2,520	0.025	141	0.076	420	0.62	2,200	1.85	5,800

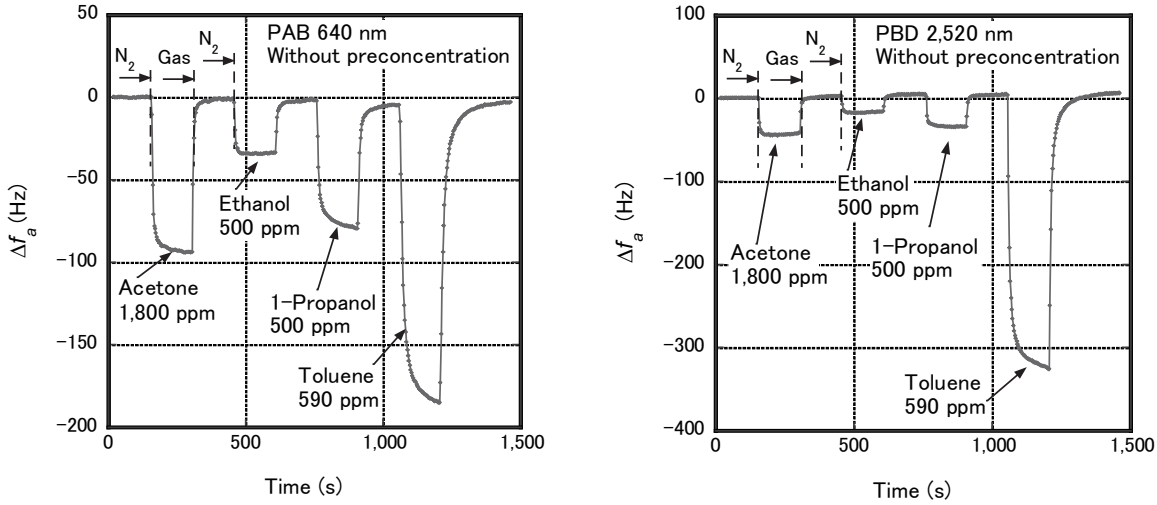

(a) (b)

Fig. 9. Frequency shift of polymer-coated cantilever for four VOCs without preconcentration: (a) 640-nm-thick PAB thin film, (b) 2,520-nm-thick PBD thin film.

by β_i (183 ppm/°C for PAB, 78 ppm/ºC for PBD) and ΔT_c measured using an on-chip p-n diode,[17] as in eq. (8). The diluted 1,800 ppm acetone, 500 ppm ethanol, 500 ppm 1-propanol, and 590 ppm toluene gases were injected in turn into the sensor chamber separated by pure nitrogen gas. These two polymers had different characteristics of sensitivity among the four VOCs: PBD has high selectivity for toluene and PAB had a relativity high sensitivity for acetone and alcohol. Figure 10 shows the concentration dependence of Δf_a among several VOCs. Then, we estimated the sensitivity s_a among VOCs, as shown in Table 1. Using eq. (6) with s_a, we also calculated the K_a for several VOCs, as shown in Table 1. For example, K_{ace} (for acetone) was 605 for PAB and 141 for PBD. K_{tol} (for toluene) was 2,650 for PAB and 2,200 for PBD. Note that K_{pxy} (for p-xylene) values for PAB and PBD was an extremely large value of 5,800. Since these K_a values are independent of t_{Poly}, f_P, and C_a, and K_a is an adequate parameter of gas adsorption selectivity for polymers.

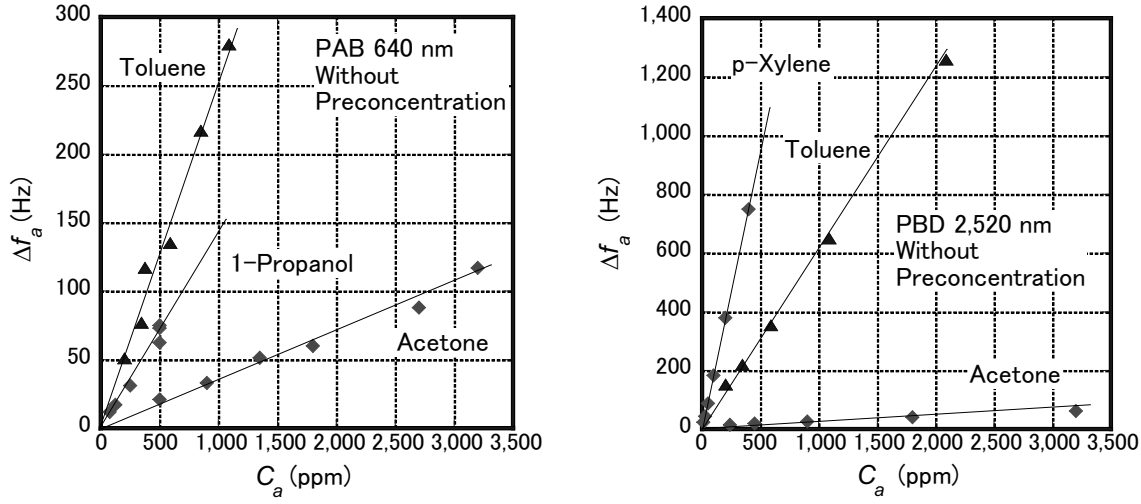

(a) (b)

Fig. 10. Frequency shift of polymer-coated cantilever for four VOCs without preconcentration: (a) 640-nm-thick PAB thin film, (b) 2,520-nm-thick PBD thin film.

3.2 *Performance of sensor system*

3.2.1 *Sensor signal from preconcentrated mixed VOCs*

To explain the analytical function of our sensor system, we evaluated the response of Δf_a from preconcentrated mixed VOCs. Two types of cantilever sensors, namely, 1) PAB of different thicknesses for acetone-toluene mixed gas and 2) PBD of different thicknesses for toluene-xylene mixed gas, are prepared and attached to a sensor system, as shown in Figs. 7(a) and 7(b). The typical conditions were as follows: V_a = 10 L (10^{-2} m^3), v_{ad} = 2.0 L/min (3.3×10^{-5} m^3/s), v_{de} = 17.2 sccm (2.86×10^{-7} m^3/s), T_r = 27ºC, and maximum preconcentrator temperature of 520°C. Figure 11(a) shows the frequency shift $\Delta f_{a,10L}$ caused by a desorbed mixed gas of acetone ($C_{ace,10L}$ = 1.8 ppm) and toluene ($C_{tol,10L}$ = 0.69 ppm), measured using two PAB-coated cantilever sensors with different thicknesses (t_{Poly} = 330 and 640 nm). The response curves had two distinct peaks corresponding to acetone and toluene. Figure 11(b) shows $\Delta f_{a,10L}$ due to the desorbed mixed gas of toluene ($C_{tol,10L}$ = 0.69 ppm) and p-xylene ($C_{pxy,10L}$ = 0.5 ppm) measured using three PBD-coated cantilever sensors with different thicknesses (t_{Poly} = 620, 1,060, and 2,520 nm). Three response curves with two peaks were also distinguished, and the peak values of $\Delta f_{a,10L}$ for the different thicknesses were proportional to t_{Poly}. We could evaluate the response of the desorption gas at the same time using a multiple cantilever system in a preset method for phase and frequency, as shown in Fig. 5.

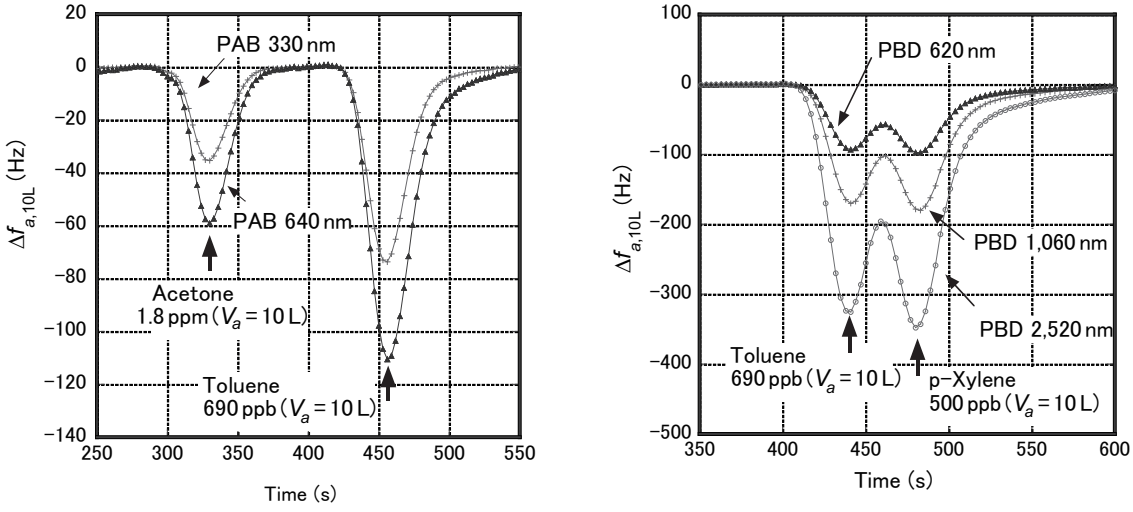

Fig. 11. Desorption responses of polymer-coated cantilevers for VOCs with preconcentrator: (a) acetone and toluene using PAB-coated sensor, (b) toluene and p-xylene using PBD-coated sensor.

3.2.2 *Estimations of preconcentration factor, efficiency, and desorption temperature*

To estimate several important parameters, including preconcentration factor $F_{a,10L}$ and system efficiency $\xi_a\eta_a$ shown in eqs. (16) to (18), the v_{de} dependences of Δf_a was evaluated. The prepared samples were described in § 2.2.1 and § 2.2.2, and the polymers were PAB (t_{Poly} = 640 nm) and PBD (t_{Poly} = 2,520 nm). Figure 12 shows the v_{de} dependences of $F_{a,10L}$ and $\xi_a\eta_a$ of (a) acetone for PAB and (b) toluene for PBD. $F_{a,10L}$ was calculated using eq. (18), and $\xi_a\eta_a$ was calculated from the mass of detected VOCs $m_{m,de}$ using eqs. (16) and (17). Although $\xi_a\eta_a$ was almost constant from 0.7 to 0.9 for v_{de} = 3 to 68 sccm, $F_{a,10L}$ decreased while v_{de} increased. We considered that the response time of $\Delta f_{a,10L}$ from VOC sensing might be an important parameter of this phenomenon because a small v_{de} rendered $\Delta f_{a,10L}$ high. The lower the v_{de} produced, the higher the $F_{a,10L}$; however, it made the width of the peaks (or deviation of Gaussian curve κ_a; we neglected j when j = 1) large and gave poor separation capability among VOCs. Here, κ_a was estimated by parameter fitting of the Gaussian curve using eq. (15) with j = 1. Thus, we decided that an adequate v_{de} was 17.2 sccm (2.8×10^{-5} m^3/s). In this case, the typical κ_a was 12 to 13 s for four VOCs. Taking the $1/v_{de}$ dependence of t_{Pa} and using eq. (13), we can estimate the desorption temperature T_a at $1/v_{de}$ = 0 for each VOC. Table 2 shows several important values estimated from the v_{de} dependence of $\Delta f_{a,10L}$, including T_a, $\xi_a\eta_a$, $F_{a,10L}$, κ_a, and t_{Pa} at v_{de} = 17.2 sccm. The maximum $F_{a,10L}$ was 910 for acetone with 640 nm PAB and 2,520 nm PBD, and the minimum was 460 for p-xylene with 2,520 nm PBD.

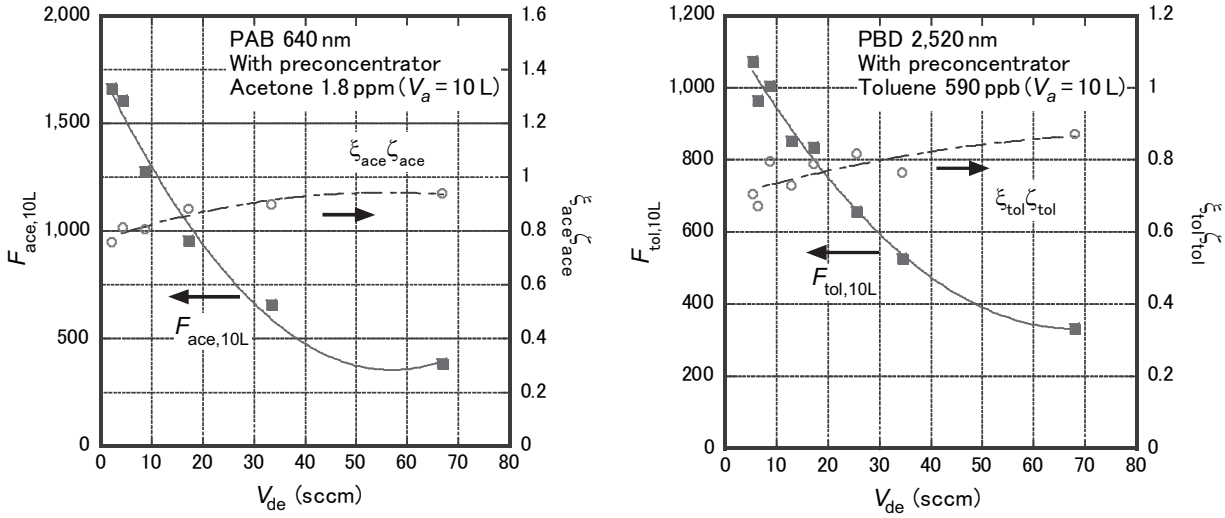

(a) (b)

Fig. 12. Concentration factor and total system efficiency for our system: (a) acetone using PAB-coated sensor, (b) toluene using PBD-coated sensor.

Table 2
System sensitivities, efficiency and detection limit for VOCs for PAB- and PBD-coated cantilevers.

Item	Unit	PAB 640 nm			PBD 2,520 nm		
		Acetone	1-Propanol	Toluene	Acetone	Toluene	p-Xylene
T_a	ºC	132	138	275	131	276	325
Sensitivity s_a	Hz/ppm	0.036	0.15	0.25	0.025	0.62	1.85
System sensitivity $S_{a,10L}$	Hz/ppm (V_a = 10 L)	32.7	88.5	148	22.7	514	850
$F_{a,10L}$ (v_{de} = 17.2 sccm)	(V_a = 10 L)	910	590	590	910	830	460
$\xi_a\eta_a$ (v_{de} = 17.2 sccm)		0.88	0.53	0.6	0.8	0.78	0.45
κ_a (v_{de} = 17.2 sccm)	s	12.2	11.5	12.9	11.9	12.6	13
t_{Pa} (t_0 = 179 s, v_{de} = 17.2 sccm)	s	327.5	345.7	456	320.6	446.6	493.1
Standard deviation λ	Hz	0.13	0.13	0.13	0.11	0.11	0.11
$DL_{a,10L}$	ppb (V_a = 10 L)	12	4.4	2.6	14.5	0.6	0.4

3.2.3 *Estimation of system sensitivity*

To estimate the system sensitivity S_a described by eq. (19), the $C_{a,10L}$ dependence of $\Delta f_{a,10L}$ was measured for the same samples as in the previous section. Figure 13 shows the $C_{a,10L}$ dependence of $\Delta f_{a,10L}$ of (a) the PAB-coated cantilever for acetone, 1-propanol, and toluene, and (b) the PBD-coated cantilever for toluene and p-xylene. The tangent of the straight line for each VOC was $S_{a,10L}$, and is listed in Table 2. The maximum $S_{a,10L}$ was 850 Hz/ppm when V_a = 10 L for p-xylene with 2,520 nm PBD and the minimum was 22.7 for acetone with 2,520 nm PBD.

As final results, we estimated the detection limit $DL_{a,10L}$ using eq. (20). A standard deviation λ was calculated with 11 points (for 33 s) of Δf_a at the same time of measurement. The estimated values were 12 ppb for acetone, 0.6 ppb for toluene, and 0.4 ppb for p-xylene, as shown in Table 2.

3.2.4 *Separation of acetone and 1-propanol using two-Gaussian model*

We tried to estimate the concentrations of acetone and 1-propanol from a mixed gas sample by fitting of two Gaussian curves using a PAB (t_{Poly} = 640 nm)-coated cantilever sensor. Since T_{ace} (for acetone) = 132ºC and T_{pnl} (for 1-propanol) = 138ºC were similar, it was very difficult to distinguish the peaks on the response curve. Therefore, we used eq. (15) to explain the actual response curve, taking account of adequate fitting parameters. Although eq. (15) has three fitting parameters ($\Delta f_{Pa,j}$, $t_{Pa,j}$, and $\kappa_{a,j}$) for each Gaussian function, $t_{Pa,j}$ and $\kappa_{a,j}$ should be constant, and only $\Delta f_{Pa,j}$ can be varied for estimating the quantitative value of $C_{a,10L}$. Figure 14 shows the fitting result to decompose two

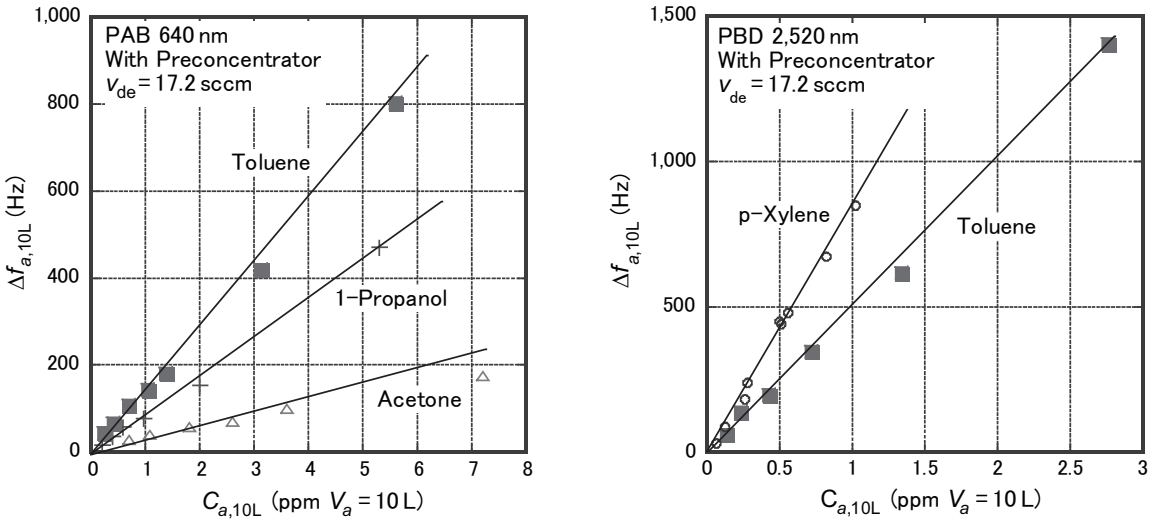

(a) (b)

Fig. 13. Frequency shift of polymer-coated cantilever for four VOCs with preconcentrator: (a) 640-nm-thick PAB thin film, (b) 2,520-nm-thick PBD thin film.

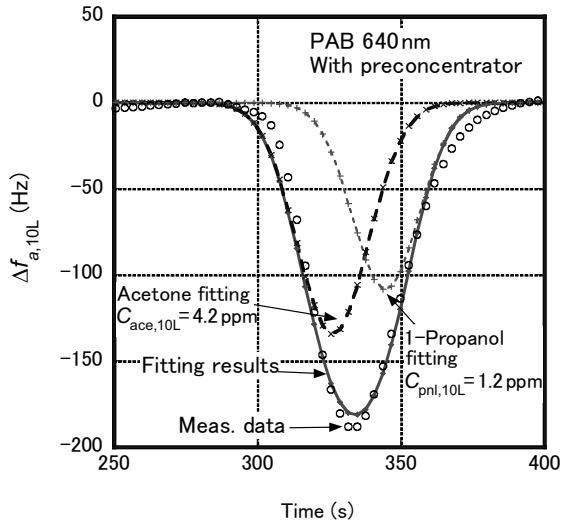

Fig. 14. Decomposition results using two Gaussian curve fittings with parameters shown in Table 2.

Gaussian curves for acetone and 1-propanol. The actual $C_{a,10L}$ values of mixed gas were $C_{ace,10L}$ = 3.6 ppm and $C_{pnl,10L}$ = 1.0 ppm, but the calculated values were 4.2 and 1.2 ppm, respectively. These discrepancies of 20% were inferred to be derived from the accuracy of $F_{a,10L}$ at low concentration.

4. Discussion

The design, structure and experimental results of a compact chemical sensor system employing polymer-coated multiple-cantilever-type mass sensors were presented. This sensor system had two merits for actual applications: (1) high sensitivity and (2) analytical function.

4.1 *High sensitivity*

High sensitivity was achieved using a preconcentrator of 6.35 mm diameter, an air pump with a large flow rate of 2.0 L/min, and a small sensor chamber of 0.3 cc. A 10 L sample of VOC was concentrated for 5 min and a 60 L volume sample for 30 min for practical application. This large sample volume made the concentration factor high. A textile structure of carbon fiber as the preconcentration material was also distributed to accomodate a large sample volume. The sensitivity, concentration factor, and detection limit for the 10 L toluene sample during 5 min of pumping were 514 Hz/ppm, and 830 and 0.6 ppb, respectively. For the 60-L sample in 30 min pumping, they were 3,084 Hz/ppm,

4,980 and 0.1 ppb, respectively. It is considered that the detection limit for actual application is 3 to 5 times larger than the estimated one. Since the indoor concentration guideline values of chemicals are 70 ppb for toluene and 200 ppb for xylene in Japan,[20] these detection limits of our chemical sensor system are good enough for monitoring these environmental solvents in a room.

4.2 *Analytical function*

This system is capable of analysis by two methods: (a) measurement of peak delay time of sensor response caused by desorption temperature difference of heated preconcentrator and (b) by the use of multiple cantilever sensors with different polymers. Our system was capable of distinguishing toluene and p-xylene from the difference in peak times. Even though the peak times of the two VOCs were similar, the concentrations of the two were estimated by parameter fitting of multiple Gaussian functions from an actual response curve. We confirmed the decomposition of the acetone and 1-propanol mixed sample by these methods. A key to the operation of multiple cantilevers was to install circuits preset for resonance frequency and feedback phase at cantilever switching by MPX. Since the resonant frequency varied with the thickness of polymer and the feedback phase varied with the site of the cantilever in a chip, it was very difficult to achieve an adequate oscillation with multiple cantilevers with different thicknesses and different polymers.

In this work, we integrated eight microcantilevers including stress gauges and a p-n diode as a temperature sensor on a chip, and four cantilevers among them were operated by multiplexing. Other electronic circuits consisted of discrete parts, operational amplifiers, ICs, and microcomputers. In the future, all electronic circuits will be integrable on the same silicon chip, as well as cantilevers, and will act as smart sensors with various intelligent functions. We also consider this system to be the first compact chemical sensor system using a MEMS mass-sensitive resonator for the purpose of environmental monitoring.

5. Conclusions

We developed a highly sensitive compact chemical sensor system employing a polymer-coated microcantilever sensor array and a thermal preconcentrator. The design, structure, and experiment results were reported. This sensor system had 1) a sub-ppb detection limit owing to concentration by a preconcentrator and 2) analytical functions enabled by thermal desorption of the preconcentrator and multiple cantilevers (acting as mass sensor) with different polymers. The preconcentration factor and system efficiency of sensing were estimated to be 830 and 0.78, respectively, for toluene. The estimated detection limit of the sensor system was less than 1 ppb for toluene and p-xylene with a 10 L sample volume, which is good enough for application to environmental monitoring. The separate detection of the mixed toluene and p-xylene was also achieved in the form of different time peaks during the heating preconcentrator operation.

Acknowledgment

This research was supported by the Regional Innovation Cluster Program of Nagano, through funds granted by the Ministry of Education, Culture, Sports, Science and Technology (MEXT), Japan.

References

1 M. Maute, S. Raible, F. E. Prins, D. P. Kern, H. Ulmer, U. Weimar and W. Goepel: Sens. Actuators, B **58** (1998) 505.
2 H. P. Langa, M. K. Ballera, R. Berger, C. Gerber, J. K. Gimzewski, F. M. Battiston, P. Fomaro, J. P. Ramseyer, E. Meyer and H. J. Giintherodt: Anal. Chim. Acta **393** (1999) 59.
3 D. Lange, C. Hagleitner, A. Hierlemann, O. Brand and H. Baltes: Anal. Chem. **74** (2002) 3084.
4 I. Dufour and L. Fadel: Sens. Actuators, B **91** (2003) 353.
5 T. Ikehara, J. Lu, M. Konno, R. Maeda and T. Mihara: J. Micromech. Microeng. **17** (2007) 2491.
6 J. Lu, T. Ikehara, Y. Zhang, R. Maeda and T. Mihara: Jpn. J. Appl. Phys. **45** (2006) 8795.
7 Y. Liu, T. Mihara, M. Kimura, M. Takasaki and T. Hirai: Proc. 24th Sensor Symp. (The Institute of Electrical Engineers of Japan, Tokyo, 2007) p. 309.
8 T. Mihara, T. Ikehara, J. Lu, R. Maeda, T. Fukawa, M, Kimura, Y. Liu and T. Hirai: Proc. 12th Int. Mtg. on Chemical Sensors (Sensor Division of the Electrochemical Society, Columbus Ohio, 2008) p. 533.
9 T. Mihara, T. Ikehara, J. Lu, R. Maeda, T. Fukawa and M. Kimura: Olfaction and Electronic Nose: Proc. 13th Int. Symp. (American Institute of Physics, Conference Proceedings, Brescia, 2009) p. 79.
10 T. Mihara, T. Ikehara, J. Lu, R. Maeda, T. Fukawa, M. Kimura, Y. Liu and T. Hirai: Proc. 25th Sensor Symp. (The Institute of Electrical Engineers of Japan, Okinawa, 2008) p. 591.
11 T. Mihara, T. Ikehara, M. Konno, R. Maeda, M. Kimura and T. Fukawa: IEEJ Trans. SM **130** (2010) 275 (in Japanese).
12 W. A. Groves, E. T. Zellersa and G. C. Fryec: Anal. Chim. Acta **371** (1998) 131.
13 F. Bender, N. Barie, G. Romoudis, A. Voigt and M. Rapp: Sens. Actuators, B **93** (2003) 135.
14 T. Nakamoto, K. Sukegawa and E. Sumitomo: IEEE Sens. J. **5** (2005) 68.
15 M. J. Henderson, B. A. Karger and G. A. Wrenshall: Diabetes **1** (1952) 188.
16 R. D. Blevins: *Formulas for Natural Frequency and Mode Shape* (Krieger Publishing, Malabar, 1979) Chapter 8, p. 108.
17 T. Ikehara, M. Konno, S. Murakami, T. Fukawa, M. Kimura and T. Mihara: Sens. Mater., 23 (2011) 381.
18 P. A. Redhead: Vacuum **12** (1962) 203.
19 M. Kimura, Y. Liu, R. Sakai, S. Sato, T. Hirai, T. Fukawa and T. Mihara: Sens. Mater., 23 (2011) 419.
20 Guideline and standard evaluation method of the VOC indoor concentration in room: Japanese Ministry of Health, Labour and Welfare, Tokyo (2000) (in Japanese).